PROCEEDINGS OF SCIENCE

LHC differential top-quark pair production cross sections in the ABMP16 PDF fit

S. Alekhin,[a] **M. V. Garzelli,**[a] **S.-O. Moch**[a] **and O. Zenaiev**[a,*]

[a] *II. Institut für Theoretische Physik, Universität Hamburg*
Luruper Chaussee 149, D–22761 Hamburg, Germany
E-mail: sergey.alekhin@desy.de, maria.vittoria.garzelli@desy.de, sven-olaf.moch@desy.de, oleksandr.zenaiev@desy.de

We investigate the impact of recent LHC measurements of differential top-quark pair production cross sections on the proton parton distribution functions (PDFs) using the ABMP16 methodology. The theoretical predictions are computed at NNLO QCD using the state-of-the-art MATRIX framework. The top-quark mass and strong coupling constant are free parameters of the fit, and we pay particular attention to the values of these parameters and their correlation as obtained from variants of the fit using different input datasets. We discuss the compatibility of different datasets and the compatibility of the fitted PDFs with those extracted from other datasets in the global ABMP16 fit, as well as with other modern global PDF sets.

42nd International Conference on High Energy Physics (ICHEP2024)
18-24 July 2024
Prague, Czech Republic

*Speaker

PoS(ICHEP2024)376

In our work [1], we provide a simultaneous fit of the parton distribution functions (PDFs), $\overline{\text{MS}}$ top-quark mass, $m_t(m_t)$, and strong coupling constant, $\alpha_s(M_Z)$, at next-to-next-to-leading order (NNLO) in the $\overline{\text{MS}}$ scheme using double-differential data on top-quark pair production, following the next-to-leading (NLO) fits already published by the CMS experimental collaboration in Ref. [2] and by us in our previous work [3], the previous ABMP16 PDF fit [5] and the approximate NNLO fit by Ref. [4]. We use the ABMP16 fit methodology, extensively described in Ref. [5]. For the double-differential $t\bar{t} + X$ distributions we used a customized version of `MATRIX` [6] interfaced to `PineAPPL` [7], as described in detail in our previous work [8].

The new PDF fit is named ABMPtt. It includes updated results for the absolute total cross sections for $t\bar{t}+X$ hadroproduction at the Tevatron and the LHC [9–18], besides all data on DIS, DY, etc. of the ABMP16 fit. Furthermore, the fit includes updated data on single-top hadroproduction in the s- and t-channel from the Tevatron [19] and in the t-channel from the LHC [20–22]. Finally, the fit includes the available datasets of normalized cross sections double-differential in $M(t\bar{t})$ and $y(t\bar{t})$ at $\sqrt{S} = 13$ TeV [2, 14, 23, 24].

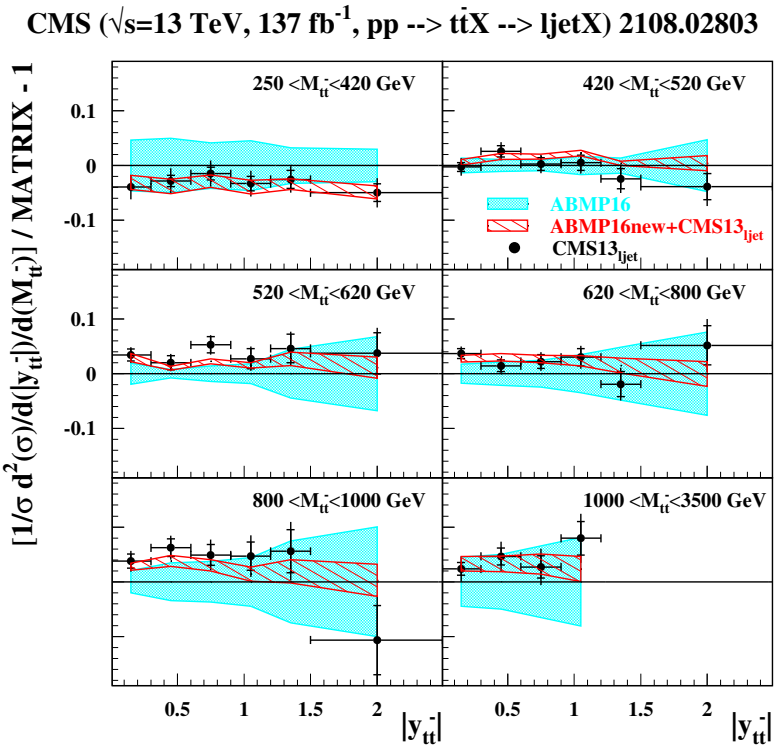

Figure 1: Pulls of CMS semileptonic data from the analysis of Ref. [14] with respect to predictions using as input ABMP16 PDFs (light-blue solid band) and the fit including besides all ABMP16 datasets the specific double-differential cross-section dataset indicated (red dashed band).

As an example, the pulls of the double-differential cross-section data collected in the $t\bar{t} + X$ CMS semileptonic analysis are shown in Fig. 1, with respect to theory predictions using as input the original ABMP16 PDF fit, and an ABMPtt fit variant obtained after including only the specific dataset. The uncertainty band on the pulls computed with the new fit turns out to be smaller than

the ABMP16 one by about a factor of two.

Experiment	Dataset	$\sqrt{s}$ (TeV)	NDP	χ^2		
				I	II	III
ATLAS	ATLAS13$_{ljet}$	13	19	34.0 (42.8)	28.2	–
	ATLAS13$_{had}$	13	10	11.9 (11.7)	11.6	–
CMS	CMS13$_{ll}$	13	15	20.7 (15.9)	–	19.6
	CMS13$_{ljet}$	13	34	44.3 (52.0)	–	42.4

Table 1: The values of χ^2 obtained for various $t\bar{t}+X$ datasets included in different variants of the present analysis (column I: variant including both ATLAS and CMS double-differential cross-section datasets; column II: variant including only ATLAS ones; column III: variant including only CMS ones). The figures in parenthesis give the values of χ^2 obtained for the corresponding dataset using as input the central ABMP16 PDFs without re-fit.

We consider different fit variants, as detailed in Table 1. In particular, in the analyses where the two ATLAS datasets are included (column II) or the two CMS datasets are included (column III), the χ^2 values slightly worsen with respect to the cases of including only a single dataset at a time (not explicitly shown here). Nevertheless, we always observe reasonable values of χ^2, as compared to the number of data points (NDP).

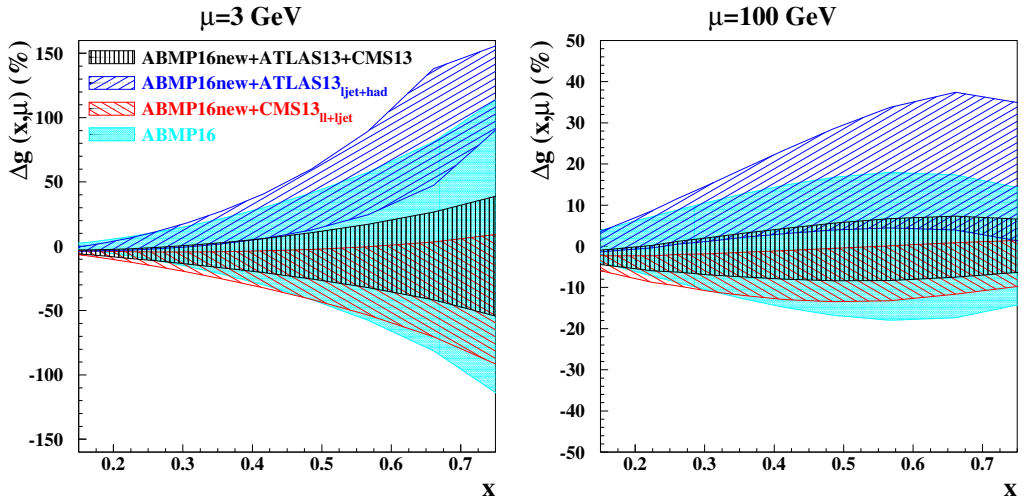

Figure 2: Percentage difference of the gluon PDF as a function of x for the variants of the ABMPtt fit of Table 1, including ATLAS $t\bar{t}+X$ double-differential cross-section datasets (right-tilted hatched area), CMS ones (left-tilted hatched areas), or both (vertical hatched area) and ABMP16 used as reference (light-blue solid area). The left panel refers to factorization scale $\mu = 3$ GeV, and the right panel refers to $\mu = 100$ GeV.

In Fig. 2 we plot the percentage differences between the gluon distributions extracted from the variants analyzed in Table 1 and the ABMP16 one as a function of x at the starting scale $\mu = 3$ GeV and evolved to $\mu = 100$ GeV. The gluon distributions in the ABMPtt fit variants are compatible with the ABMP16 one, and present uncertainties decreased by a factor ~ 2 with respect to ABMP16 in the large x region, $x \gtrsim 0.1$. The simultaneous determination of the PDFs, $m_t(m_t)$ and $\alpha_s(M_Z)$ in

the ABMPtt global fit leads to the value of $\alpha_s(M_Z)$ in the $n_f = 5$ flavor scheme at NNLO

$$\alpha_s^{(n_f=5)}(M_Z) \quad = \quad 0.1150 \pm 0.0009\,, \tag{1}$$

which is very similar, both in terms of central value, and in terms of uncertainty, to the ABMP16 one 0.1147 ± 0.0008. For the top-quark mass in the $\overline{\text{MS}}$ scheme we obtain at NNLO the best-fit value

$$m_t(m_t) \quad = \quad 160.6 \pm 0.6 \text{ GeV}\,, \tag{2}$$

which is also well compatible with the ABMP16 one 160.9 ± 1.1 GeV, and with uncertainties reduced by a factor of approximately two. As an illustration of the correlation between the $m_t(m_t)$

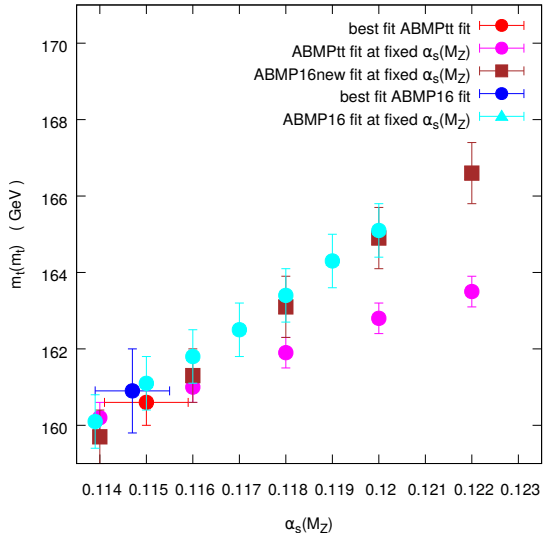

Figure 3: Values of $m_t(m_t)$ (extracted together with the PDFs) at fixed $\alpha_s(M_Z)$, for the ABMP16 and the ABMPtt fits. The best fit values of $m_t(m_t)$ and $\alpha_s(M_Z)$ are also shown in both cases for the most general analyses, where also $\alpha_s(M_Z)$ is allowed to vary simultaneously with the PDFs and $m_t(m_t)$.

and $\alpha_s(M_Z)$ values, in Fig. 3 one can see an approximately linear increase of $m_t(m_t)$ with $\alpha_s(M_Z)$, with a correlation coefficient decreased with respect to the ABMP16 fit.

The ABMPtt PDFs are available as grids in the format of the `LHAPDF` library [25] and available under `https://lhapdf.hepforge.org/pdfsets`. For a fixed number of flavors, $n_f = 3, 4$ and 5, at NNLO, the grids are named `ABMPtt_3_nnlo` (0+29), `ABMPtt_4_nnlo` (0+29), `ABMPtt_5_nnlo` (0+29), and contain the central fit (set 0) together with additional 29 sets for the combined symmetric PDF uncertainties (including variations of the values of α_s and the heavy-quark masses). The latter correspond to $\pm 1\sigma$-variations. The `LHAPDF` grids contain values of the heavy-quark masses. The PDF set with three light-quark flavors `ABMPtt_3_nnlo` is valid at all perturbative scales $\mu \geq 1$ GeV, whereas the PDFs sets for $n_f = 4$ or 5, `ABMPtt_4_nnlo` or `ABMPtt_5_nnlo`, are only meaningful at scales, which are much larger than the charm- or bottom-quark masses.

In summary, we have shown that the use of state-of-the-art data on absolute total inclusive and normalized cross sections double differential in $M(t\bar{t})$ and $y(t\bar{t})$ in a simultaneous NNLO fit of PDFs, $\alpha_s(M_Z)$ and $m_t(m_t)$ following the ABMP methodology, leads to a reduction of the

uncertainties by a factor ~ 2 on both the gluon PDF and the $m_t(m_t)$ value, with respect to the previous ABMP16 fit. The value of $\alpha_s(M_Z)$ remains essentially unchanged, but its correlation with the top-quark mass is decreased. The resulting PDFs are publicly available as grids in the format of the `LHAPDF` library.

References

[1] S. Alekhin, M.V. Garzelli, S.O. Moch and O. Zenaiev, *NNLO PDFs driven by top-quark data*, 2407.00545.

[2] CMS collaboration, *Measurement of* $\mathrm{t\bar{t}}$ *normalised multi-differential cross sections in pp collisions at* $\sqrt{s} = 13$ *TeV, and simultaneous determination of the strong coupling strength, top quark pole mass, and parton distribution functions*, *Eur. Phys. J. C* **80** (2020) 658 [1904.05237].

[3] M.V. Garzelli, L. Kemmler, S. Moch and O. Zenaiev, *Heavy-flavor hadro-production with heavy-quark masses renormalized in the* $\overline{\mathrm{MS}}$*, MSR and on-shell schemes*, *JHEP* **04** (2021) 043 [2009.07763].

[4] M. Guzzi, K. Lipka and S.-O. Moch, *Top-quark pair production at hadron colliders: differential cross section and phenomenological applications with DiffTop*, *JHEP* **01** (2015) 082 [1406.0386].

[5] S. Alekhin, J. Blümlein, S. Moch and R. Placakyte, *Parton distribution functions,* α_s*, and heavy-quark masses for LHC Run II*, *Phys. Rev. D* **96** (2017) 014011 [1701.05838].

[6] M. Grazzini, S. Kallweit and M. Wiesemann, *Fully differential NNLO computations with MATRIX*, *Eur. Phys. J. C* **78** (2018) 537 [1711.06631].

[7] S. Carrazza, E.R. Nocera, C. Schwan and M. Zaro, *PineAPPL: combining EW and QCD corrections for fast evaluation of LHC processes*, *JHEP* **12** (2020) 108 [2008.12789].

[8] M.V. Garzelli, J. Mazzitelli, S.O. Moch and O. Zenaiev, *Top-quark pole mass extraction at NNLO accuracy, from total, single- and double-differential cross sections for* $t\bar{t} + X$ *production at the LHC*, *JHEP* **05** (2024) 321 [2311.05509].

[9] CDF, D0 collaboration, *Combination of Measurements of the Top-Quark Pair Production Cross Section from the Tevatron Collider*, *Phys. Rev. D* **89** (2014) 072001 [1309.7570].

[10] CMS collaboration, *Measurement of the inclusive* $\mathrm{t\bar{t}}$ *production cross section in proton-proton collisions at* $\sqrt{s} = 5.02$ *TeV*, *JHEP* **04** (2022) 144 [2112.09114].

[11] ATLAS collaboration, *Measurement of the* $t\bar{t}$ *production cross-section in pp collisions at* $\sqrt{s}$ *= 5.02 TeV with the ATLAS detector*, *JHEP* **06** (2023) 138 [2207.01354].

[12] ATLAS, CMS collaboration, *Combination of inclusive top-quark pair production cross-section measurements using ATLAS and CMS data at* $\sqrt{s} = 7$ *and 8 TeV*, *JHEP* **07** (2023) 213 [2205.13830].

[13] CMS collaboration, *Measurement of the* $\mathrm{t\bar{t}}$ *production cross section, the top quark mass, and the strong coupling constant using dilepton events in pp collisions at* $\sqrt{s}$ *= 13 TeV*, *Eur. Phys. J. C* **79** (2019) 368 [1812.10505].

[14] CMS collaboration, *Measurement of differential* $t\bar{t}$ *production cross sections in the full kinematic range using lepton+jets events from proton-proton collisions at* $\sqrt{s}$ *= 13 TeV*, *Phys. Rev. D* **104** (2021) 092013 [2108.02803].

[15] ATLAS collaboration, *Measurement of the* $t\bar{t}$ *production cross-section in the lepton+jets channel at* $\sqrt{s}$ = 13 *TeV with the ATLAS experiment*, *Phys. Lett. B* **810** (2020) 135797 [2006.13076].

[16] ATLAS collaboration, *Inclusive and differential cross-sections for dilepton* $t\bar{t}$ *production measured in* $\sqrt{s}$ *= 13 TeV pp collisions with the ATLAS detector*, *JHEP* **07** (2023) 141 [2303.15340].

[17] CMS collaboration, *First measurement of the top quark pair production cross section in proton-proton collisions at* $\sqrt{s}$ *= 13.6 TeV*, *JHEP* **08** (2023) 204 [2303.10680].

[18] ATLAS collaboration, *Measurement of the* $t\bar{t}$ *cross section and its ratio to the Z production cross section using pp collisions at* $\sqrt{s}$*=13.6 TeV with the ATLAS detector*, *Phys. Lett. B* **848** (2024) 138376 [2308.09529].

[19] CDF, D0 collaboration, *Tevatron Combination of Single-Top-Quark Cross Sections and Determination of the Magnitude of the Cabibbo-Kobayashi-Maskawa Matrix Element* $\mathbf{V_{tb}}$, *Phys. Rev. Lett.* **115** (2015) 152003 [1503.05027].

[20] ATLAS, CMS collaboration, *Combinations of single-top-quark production cross-section measurements and* $|f_{LV}V_{tb}|$ *determinations at* $\sqrt{s}$ *= 7 and 8 TeV with the ATLAS and CMS experiments*, *JHEP* **05** (2019) 088 [1902.07158].

[21] CMS collaboration, *Measurement of the single top quark and antiquark production cross sections in the t channel and their ratio in proton-proton collisions at* $\sqrt{s}$ *= 13 TeV*, *Phys. Lett. B* **800** (2020) 135042 [1812.10514].

[22] ATLAS collaboration, *Measurement of t-channel production of single top quarks and antiquarks in pp collisions at 13 TeV using the full ATLAS Run 2 dataset*, .

[23] ATLAS collaboration, *Measurements of top-quark pair differential and double-differential cross-sections in the* ℓ*+jets channel with pp collisions at* $\sqrt{s}$ = 13 *TeV using the ATLAS detector*, *Eur. Phys. J. C* **79** (2019) 1028 [1908.07305].

[24] ATLAS collaboration, *Measurements of top-quark pair single- and double-differential cross-sections in the all-hadronic channel in pp collisions at* $\sqrt{s}$ = 13 *TeV using the ATLAS detector*, *JHEP* **01** (2021) 033 [2006.09274].

[25] A. Buckley, J. Ferrando, S. Lloyd, K. Nordström, B. Page, M. Rüfenacht et al., *LHAPDF6: parton density access in the LHC precision era*, *Eur. Phys. J. C* **75** (2015) 132 [1412.7420].